Mechanism of direct current electrical charge conduction in p-toluenesulfonate doped polypyrrole/carbon composites

Amit Kumar, Rajiv K. Singh, Hari K. Singh, Pankaj Srivastava, and Ramadhar Singh

Citation: Journal of Applied Physics **115**, 103702 (2014); doi: 10.1063/1.4868088
View online: http://dx.doi.org/10.1063/1.4868088
View Table of Contents: http://scitation.aip.org/content/aip/journal/jap/115/10?ver=pdfcov
Published by the AIP Publishing

Mechanism of direct current electrical charge conduction in *p*-toluenesulfonate doped polypyrrole/carbon composites

Amit Kumar,[1,2] Rajiv K. Singh,[1] Hari K. Singh,[1] Pankaj Srivastava,[2] and Ramadhar Singh[1,a)]
[1]*National Physical Laboratory, Council of Scientific and Industrial Research, Dr. K. S. Krishnan Marg, New Delhi 110012, India*
[2]*Department of Chemistry, Banaras Hindu University, Varanasi 221005, India*

(Received 17 January 2014; accepted 27 February 2014; published online 10 March 2014)

Polypyrrole/carbon (PPy/C) composites have been synthesized using varying concentration of *p*-toluenesulfonate (pTS) dopant by surface initiated *in-situ* chemical oxidative polymerization. The synthesis and influence of pTS on the structure of the PPy/C composites are confirmed by Fourier transform infrared studies and the morphological features have been examined by scanning electron microscopy. X-ray photoelectron spectroscopy, employed to examine the surface composition and doping level of these composites, confirms the anionic doping into the polymer backbone. Electron spin resonance measurement has been carried out on these samples to identify the nature of the charge carriers and their concentration at different doping levels. The dc electrical conductivity of these composites has been measured in the temperature range ~10–305 K. The observed results have been analyzed in the framework of existing theoretical models. Different Mott's parameters, such as characteristic temperature (T_0), density of states at the Fermi level {$N(E_F)$}, average hopping distance (R), and average hopping energy (W), evaluated from dc conductivity data supports the applicability of Mott's three dimensional variable range hopping mechanism in this system. © *2014 AIP Publishing LLC*. [http://dx.doi.org/10.1063/1.4868088]

I. INTRODUCTION

For more than three decades, extensive research has been carried out in relation to the synthesis, doping, spectroscopic, photophysical, and electrical characterization of conducting polymers, such as polyacetylene (PA), polypyrrole (PPy), polyaniline (PANI), polythiophene (PT), poly(*p*-phenylenevinylene) (PPV), and their derivatives, blends, or composites.[1–5] Owing to the metal-like conductivity or semi-conductivity and several other fascinating properties of conducting polymers, these materials have carved out for themselves indispensable role in variety of specialized applications such as in organic photovoltaics, organic light emitting diodes, fuel cells, supercapacitors, electromagnetic interference shielding, and biological and microbial sensors.[1–5] The ease of synthesis, combination of their electrical conductivity, and polymeric properties, such as low density, flexibility, and ease of structural modifications as well as their chemical and environmental stability, have made them good and viable alternative for the inorganic semiconductors being used currently in microelectronics. Among these conducting polymers, PPy and its derivatives, which embody several unique features, such as high conductivity, environment friendliness, low cost, and fast charge-discharge kinetics, have generated wide interest in the area of energy storage.[6–11] The characteristic redox doping-undoping process of PPy can be useful in the charge storage systems, but the simultaneous occurrence of swelling and contraction associated with this process weakens the materials stability and hence affects its long term utilization. To overcome this, an aromatic dopant *p*-toluenesulfonate (pTS) is incorporated during the synthesis of PPy/C composites to obtain a high conducting PPy/C composites with substantial amount of electrochemical and thermal stability.[12] But before such PPy/C composites could be used for device applications, it was thought worthwhile to examine in detail the mechanism of dc electrical charge conduction in this composite system.

Different conduction models, similar to those developed for amorphous semiconductors,[13] have been proposed[14–18] to explain the mechanism of dc electrical charge conduction in conducting polymers; however, the different types of structural and electronic defects as well as lack of long range ordering in these systems do not allow to explain the mechanism of charge transport completely. Kivelson[14] was first to propose a model to explain the mechanism of conduction in polyacetylene wherein the charge transport occurs between neutral and charged solitons at iso-energetic levels. This model was modified for the materials having non-degenerate ground state for inter-polaron hopping conduction.[15] The other two models, widely used to explain the dc conductivity of conjugated polymeric systems, are fluctuation induced tunneling (FIT)[16] and Mott's variable range hopping (VRH) conduction.[17–33] In FIT conduction model,[16] the tiny conducting domains, formed during doping in a granular system, participates in the delocalization of charge carriers by tunneling between conducting metallic islands. However, the macroscopic conductivity in most of the conjugated polymeric systems is assumed to result from the hopping conduction process. In the hopping conduction process, the strongly localized charge carriers hop to the nearest neighboring state and the conductivity is proportional to Boltzmann's factor $\exp(-W/k_BT)$, where k_B is Boltzmann's constant, T is the temperature, and W is the difference of energy between

a)Electronic mail: ramadhar@mail.nplindia.org

two states. W is called the hopping energy or the activation energy required by a charge carrier to hop from one state to another. However, when the carrier localization is not strong, the charge carriers jump to the sites for which the required activation energy is small and resides farther away, then the charge transport occurs by VRH.[13,23] It is worthwhile to mention here that the Mott's VRH conduction model has been applied to explain the dc conductivity of many conjugated polymeric systems such as doped polyacetylene,[25,26] polyanilines,[27,28] poly(2,5-dimethoxyaniline),[17] polypyrroles,[18,21–23,33] poly(3-methylthiophene),[29–31,34] poly(3-hexylthiophene),[19] and poly(3-octylthiophene),[20,32] carbon-black/polypyrrole nanocomposites.[35] Several studies on dc conduction of different conducting polymers and their composite systems are available in literature.[17–32] However, there is no report available on temperature dependence of dc electrical conductivity in pTS doped PPy/C composites.

In the present paper, we report a detailed investigation of dc electrical conductivity (σ_{dc}) of pTS doped PPy/C composite systems in the wide temperature range of 10–305 K. The evaluated values of different Mott's parameters provide the evidence of applicability of Mott's three dimensional (3D)-VRH conduction model in these composites. Electron spin resonance (ESR) measurement is used to estimate the spin concentration of the charge carriers involved in the conduction process.

II. EXPERIMENTAL

A. Synthesis of PPy/C composites

Different samples of pTS doped PPy/C composites were synthesized using doubly distilled pyrrole monomer (Fluka Chemie) (0.1M), ammonium peroxodisulfate (APS) (an oxidant) and *p*-toluenesulfonic acid (dopant) (MERCK), Vulcan-carbon XC-72R (particle size ~50 nm) (Cabot Corporation, Massachusetts) in an aqueous medium (de-ionized (DI) water ~18 MΩ cm) at 275 K by using *in-situ* chemical oxidative polymerization technique. The procedure for synthesis is described here in brief. First of all, 20 wt. % of acid activated Vulcan-carbon was dispersed ultrasonically in 100 ml of DI water for ~60 min to form a uniform suspension. Afterwards, pyrrole monomer (0.1M) was added to this reaction solution and was stirred under inert atmosphere (N_2) for ~30 min. APS (oxidant) was dissolved in 20 ml of DI water (molar ratio of APS:Py, 1:1) and added to the reaction solution drop-wise under constant stirring. The polymerization was made to continue under constant stirring for 8 h. This resultant PPy/C composite was then washed with copious amount of methanol and deionized water to remove any trace amount of impurities. Afterwards, the sample was successively filtered and kept overnight at ~60 °C in oven. For the synthesis of pTS doped PPy/C samples, varying concentration of pTS were added with pyrrole monomer prior to addition of oxidant (APS), keeping the rest of polymerization procedure same. The details of this have been described elsewhere.[12] All the five synthesized samples of the present investigation have been designated as S1, S2, S3, S4, and S5. The dopant concentration along with their room temperature (~300 K) dc conductivity (σ_{dc}) are given in Table I.

TABLE I. Samples nomenclature of PPy/C composites with their respective dopant concentration along with their room temperature dc conductivity (σ_{dc}) and sulfur to nitrogen (S/N) ratio.

Sample name	Pyrrole (M)	pTS (M)	DC conductivity at 300 K (S/cm)	S/N ratio from XPS analysis
S1	0.10	0.00	1.02	0.1256
S2	0.10	0.01	1.36	0.1538
S3	0.10	0.03	2.62	0.1605
S4	0.10	0.06	4.95	0.1697
S5	0.10	0.10	7.09	0.1787

B. Measurements

Fourier transform infrared (FT-IR) of these PPy/C composites: S1, S2, S3, S4, and S5 (results not shown) taken on Cary 630, IR spectrometer shows bands around 1540 and 1465 cm^{-1}, which are assigned to C=C and C-C characteristic ring vibrations of polypyrrole. The presence of pTS dopant anion in the backbone of PPy/C composite matrix has been observed by the broadening of band at 1024 cm^{-1}, which may be due to the overlapped signals of N-H with -SO_3 group. The occurrence of above mentioned bands in FT-IR spectra and reproducibility of the room temperature dc conductivity data (Table I) confirm the synthesis of pTS doped PPy/C composites used with various dopant concentration. The details regarding FT-IR and other structural investigations are available in our recent publication.[12] The surface morphology of these PPy/C composites was analyzed by using scanning electron microscope (SEM) on a Zeiss model EVO MA-10.

X-ray photoelectron spectroscopy (XPS) analysis was carried out on the PPy/C composite samples using an ESCA machine of VSW Scientific Instruments (UK) equipped with Mg and Al twin anode X-ray source. Al K(α) (resolution ~0.9 eV) was employed as the source radiation in the XPS study. The C(1s) peak was used for the calibration of the photoelectron spectrometer, while Au sample served as an external reference for resolution and binding energy (B.E.).

The ESR measurements on these PPy/C composite samples were recorded with a Brukar Biospin make model A300 EPR spectrometer operated at the X-band ($\nu = 9.6$ GHz), with 100 kHz field modulation at room temperature. For this measurement, these composite samples were kept under dynamic vacuum for 12 h in order to prevent oxygen attack. Samples of S1, S2, S3, S4, and S5 having an appropriate and equal weight were sealed in quartz capillary tubes. For recording the ESR spectra, the dc magnetic field of the spectrometer was modulated at 100 kHz and modulation amplitude was kept 1 G to avoid any distortion in ESR line shape. Microwave power was also kept very low to avoid any saturation effect. 1,1 diphenyl-2-picrylhydrazyl (DPPH) was used as a standard reference sample for calculation of g-value and spin concentration of all the samples.[36] The same spectrometer setting except different gain factors was used for recording the spectra of all the samples in the present work. The spin concentration was calculated by comparing the integrated area of the absorption curves of ESR signal obtained for known weight of each sample with that

of reference sample DPPH recorded under similar conditions.

The dc electrical conductivity (σ_{dc}) of these PPy/C composites was measured on pressed pellets using collinear four-point probe method. Temperature dependent dc electrical conductivity measurement was performed in closed cycle refrigerator (Advance Research System Inc., USA) with lakeshore 332 temperature controller in the temperature range ~10–305 K using Keithley 224 programmable current source for applying the current and Keithley 181 digital nanovoltmeter for measuring the voltage. The data were recorded in the warming cycle (~10–305 K) using a software based on LabView platform.

III. RESULTS AND DISCUSSION

A. Structural and surface morphological investigation

It is imperative to mention here that the organic counter anion pTS under the influence of π-π conjugation allows a laminar growth resulting into ordered surface morphology in the polymer.[18] Although the scanning electron micrographs of PPy/C composites (S1-S5) has been given in our recent work,[12] the same has been reported here on same magnification for showing its correlation with ESR, XPS, and dc conductivity results. The surface morphology of PPy/C composites; S1, S2, S3, S4, and S5 given in Figs. 1(a)–1(e), shows the polymer growth on carbon particles. The polymer-carbon composite shows porous architecture, wherein small globular features of inter-connected polymer/carbon spheres are seen. The impact of pTS addition can be seen in the increase of radius of these polymer/carbon spheres. This enhanced polymer-polymer network can be associated with the large aromatic organic dopant anion pTS, since the addition of pTS affects the π-π interaction between the dopant and the conjugated backbone of the polymer. This altogether increases the conjugation length which in turn has an impact on increasing the electrical conductivity of the polymer. The large and diffused network of PPy/C spheres is supported by the microstructural features observed in TEM micrographs.[12] It has been found that the formation of conduction channel inside the polymer matrix affects the effective transfer of charges across the electrode/electrolyte interface through polaronic and bipolaronic species. Hence, the formation of conduction channel or the polaronic and bipolaronic species

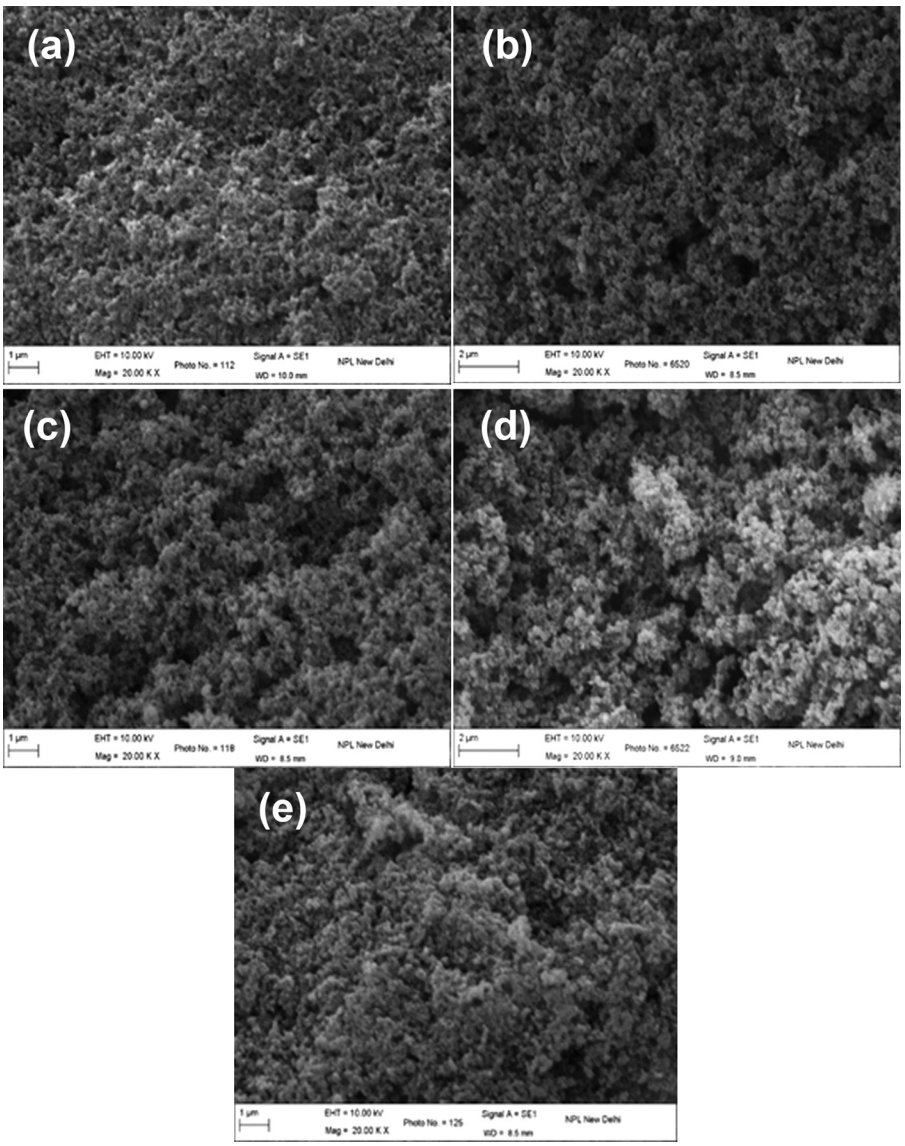

FIG. 1. SEM images of PPy/C samples: (a) S1 (b) S2, (c) S3, (d) S4, (e) S5.

has been further explored using XPS and ESR spectroscopic investigations and discussed in Secs. III B and III C.

B. X-ray photoelectron spectroscopy

To understand the role of nitrogen and sulfur functionalities in the capacitive performance of the material for electrodes, it is important to elucidate the types of nitrogen present on the carbon surface. The binding energy with their respective bond assignments and the chemical composition of the surface of these chemically synthesized PPy/C composites, S1, S2, S3, S4, and S5, has been examined by XPS. The XPS survey spectra of various samples of PPy/C composites, i.e., S1, S2, S3, S4, and S5 (Fig. 2), show three prominent peaks which represents C(1s), N(1s), and O(1s) along with one additional peak of S(2 p). In the present case, C(1s), N(1s), and S(2p) peaks are of particular interest. The deconvoluted peaks through Gaussian fitting of respective high resolution core-level spectrum, i.e., C(1s), N(1s), and S(2p) are depicted in Figs. 3–5, respectively. Sulfur to nitrogen (S/N) ratio calculated from the spectral data is given in Table I.

The deconvolution of C(1s) region spectrum to identify the surface functionalities of PPy/C composites, S1, S2, S3, S4, and S5, are shown in Fig. 3. To compensate the surface charging effect, all core-level spectra are referenced with respect to C(1s) hydrocarbon peak at 284.6 eV.[37] The core level spectra in Fig. 3 have been deconvoluted into three components centered at 284.5, 286.5, and 288.8 eV. The main peak at 284.5 eV is attributed to the collective effect of C-C, C=C, and C-H. The component at 286.5 eV corresponds to C-N, C-S, and C-O contributions,[38] whereas the component at 288.8 eV is indicative of the presence of carbonyl groups.[39] The highest binding energy, indicative of carbonyl groups, arises due to the attack of water molecules during the course of polymerization.[40,41] Thus, the relative area of this peak can be used to calculate the density of carbonyl defects within the polymers.[39] It has been ascertained through peak area calculation that the amount of carbonyl defects is lower for sample S5 as compared to other synthesized composites.

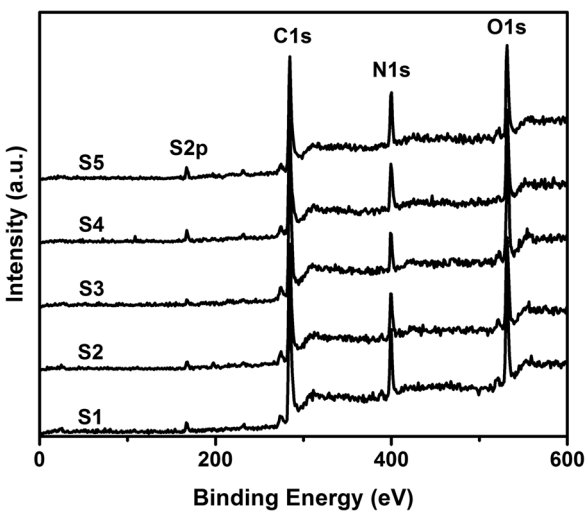

FIG. 2. XPS survey scan of the synthesized PPy/C samples: S1, S2, S3, S4, and S5, indicating the peak associated with the elements present in the composites.

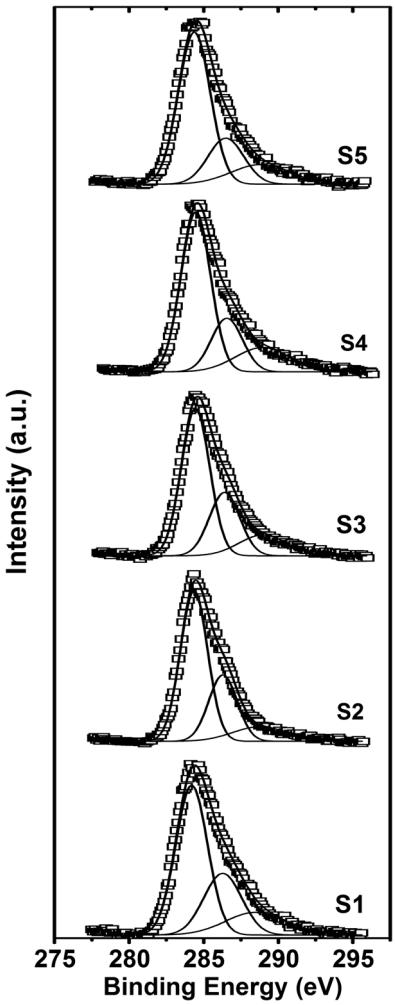

FIG. 3. High resolution XPS spectra of experimental (square) and deconvoluted (line) C(1s) peaks: S1, S2, S3, S4, and S5.

The N(1s) core level spectra (Fig. 4) dominated by a main peak at 399.5 eV are assigned to the neutral nitrogen functionalities in the polymer, i.e., −N= and -NH_2 components, whereas the peak arises at 401.2 eV is due to the protonated nitrogen atoms or high oxidation states of the nitrogen atoms.[42,43] The oxidation level of the synthesized samples has been calculated from the ratio of the peak area of protonated nitrogen atoms to that of total area of the N(1s) core spectrum. It is found that this ratio increases with increase in pTS concentration (from 0.0 to 0.1M). There is an increase in oxidation level with increasing pTS concentration. This is related to the enhanced concentration of polarons and bipolarons and could be regarded as the reason for the observed higher conductivity of the sample.[12] The variation in oxidation level is found to consistent with the room temperature dc conductivity values of the PPy/C composites.

In addition to this, a peak corresponding to sulfonated functionalities, i.e., S(2p) arises at 167.7 eV (Fig. 5). Calculation of the ratio of sulfur to nitrogen (S/N), by using the integral area of their respective core level spectra, a conclusion can be drawn on the effect of doping on the structure of the synthesized composites. The ratio S/N increases from 0.1256 to 0.1787 representing an increase in sulfur content with respect to nitrogen. This increase in sulfur content with

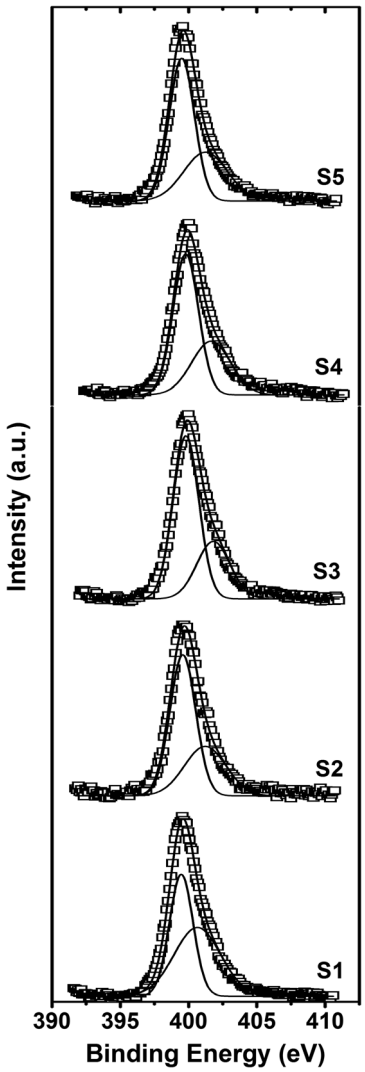

FIG. 4. High resolution XPS spectra of experimental (square) and deconvoluted (line) N(1s) peaks: S1, S2, S3, S4, and S5.

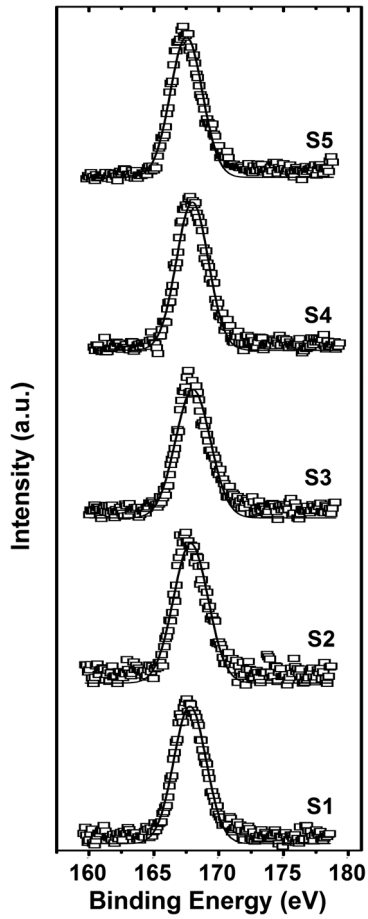

FIG. 5. High resolution XPS spectra of experimental (square) and deconvoluted (line) S(2p) peak: S1, S2, S3, S4, and S5.

increasing dopant anion concentration (pTS) favors the increase in oxidation level of the polymer.

C. ESR spectroscopy

In order to understand the impact of dopant on the polymer, a study based on ESR has been undertaken. The ESR spectrum of PPy/C sample shows a single symmetric ESR signal (Fig. 6) indicating the presence of free electron. The line shape of this narrow signal is Lorentzian-type and is almost symmetric, i.e., A/B $\sim$ 1 for all the samples. This clearly indicates that the probability of oxygen attack on these samples is very small.[44] The number of spins (Ns) is observed to increase with the increase in the concentration of the dopant pTS (Table II). This can be attributed to the increase in spin concentration of the polymer. Moreover, the increase in dc electrical conductivity of these samples shows a similar trend with the increase in intensity of this narrow ESR signal. The simultaneous appearance of these phenomena, viz., the increase in the number of spins and the electrical conductivity suggests a correlation between them. Therefore, the observed change in the ESR signal is due to charge carriers formed during doping process. The g-factor of this signal is roughly constant for all the samples and is $\sim$2.0027. This is closer to a g value (2.0023) of free electron which confirms that the resonance comes from electrons delocalized in the π-system of the carbon atoms forming polymer backbone in the main chain. It also indicates that the localization is less strong and further suggests that these charge carriers can jump to the sites for which the activation

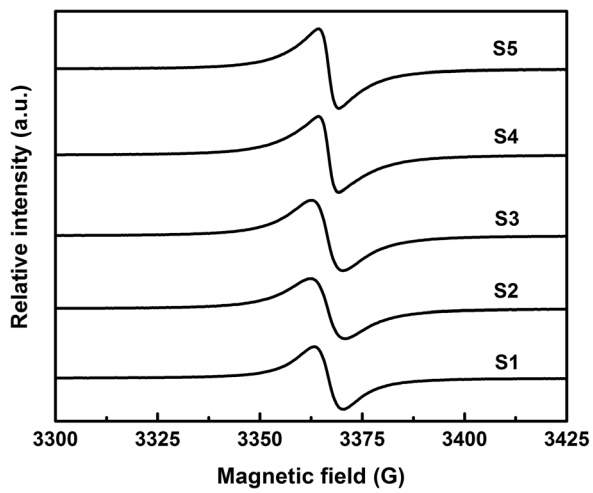

FIG. 6. ESR spectra of PPy/C composites: S1, S2, S3, S4, and S5.

TABLE II. DC conductivity (σ_{dc}) and activation energy (E_A) at 300 K and spin number (Ns (calculated from ESR spectra)), different Mott's parameters, characteristic temperature (T_0), the density of states at Fermi level ($N(E_F)$), average hooping distance (R), the average hopping energy (W), for various samples of PPy/C composites.

Samples	σ_{dc} (300 K) (S/cm)	E_A (300 K) (meV)	Ns ($\times 10^{19}$)	T_0 (K)	N (E_F) $\times 10^{20}$ ($cm^{-3}\,eV^{-1}$)	R (300 K) (Å)	W (300 K) (meV)	αR
S1	1.02	72.2	3.02	1.71×10^6	4.16	17.7	102.1	5.93
S2	1.36	65.0	3.52	1.04×10^6	6.84	15.7	90.2	5.23
S3	2.62	61.2	3.79	3.89×10^5	18.35	12.3	70.5	4.09
S4	4.95	52.9	3.86	1.63×10^5	43.72	9.9	56.7	3.29
S5	7.09	44.2	3.93	7.22×10^4	98.88	8.0	46.3	2.68

energy is smaller but reside farther away, i.e., the electrical conduction takes place by VRH.[22,23]

D. Temperature dependence of dc conductivity

Figure 7 shows the variation of log σ_{dc} as a function of reciprocal temperature in the range of 10–305 K for PPy/C composite samples: S1, S2, S3, S4, and S5. The observed trend in σ_{dc} vs. 1000/T appears similar to those reported earlier for other conjugated polymers.[17,19,20,24,27–32] The dc conductivity σ_{dc} (Fig. 7) can be given[13,45] by the following relation:

$$\sigma_{dc} = \sigma_o \exp\left[-\frac{E_A}{k_B T}\right], \quad (1)$$

where σ_o is a pre-exponential factor, E_A is the activation energy, k_B is Boltzmann's constant, and T is temperature. The observed temperature dependent dc conductivity data (Fig. 7) have been first analyzed to see the applicability of Kivelson's model.[14] In this model, the inter-chain transport occurs by hopping between neutral and charged soliton states at iso-energetic levels. The neutral solitons are mobile along the carbon chain, whereas the charged solitons are pinned next to the dopant ions. However, their roles are interchanged in the hopping process. According to this model,[14] the temperature dependence of dc conductivity can be approximated by a simple power law given as

$$\sigma = AT^n, \quad (2)$$

where A is a constant. The power index "n" lies typically around ten or above. This intersoliton model has been modified for interpolaronic hopping conduction in conducting polymers having a non-degenerate ground state wherein the hopping takes place between a polaron and bipolaron both pinned by counter ions.[15] The measured dc conductivity data for all the samples have been plotted as log σ_{dc} versus log T (Fig. 8) and the value of power index "n" is found to be in the range ~1.24–2.75 for all the samples of the present work. This shows that the Kivelson's model[14] is not applicable in the present investigation.

It is evident from ESR investigations that ESR line shape for all the PPy/C composite samples is of Lorentzian type and almost symmetric indicating thereby that the oxygen attack on these samples is negligible.[44] A single Lorentzian ESR line shape having no Dysonian asymmetry[24] rules out the possibility of formation of metallic islands thus eliminating the probability of FIT conduction[16] in these PPy/C composite samples.[23,46,47]

However, before the application of Mott's VRH conduction model[13] to explain the dc conductivity results, it was thought worthwhile to examine the temperature dependence of activation energy. For this, the activation energy at different temperatures has been evaluated from Fig. 7 and is shown in Fig. 9(a). To explain the results of the present investigation, the activation energy has been analyzed[17–19,23] by the following equation:

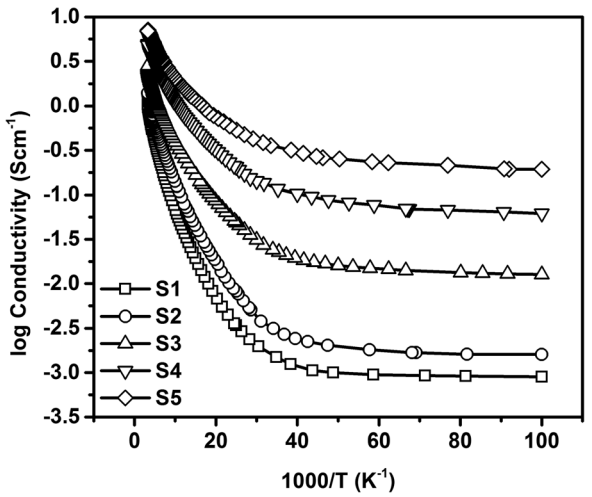

FIG. 7. Plot of log of dc conductivity (σ_{dc}) with inverse of temperature in the range of 10–305 K for various PPy/C samples: S1, S2, S3, S4, and S5.

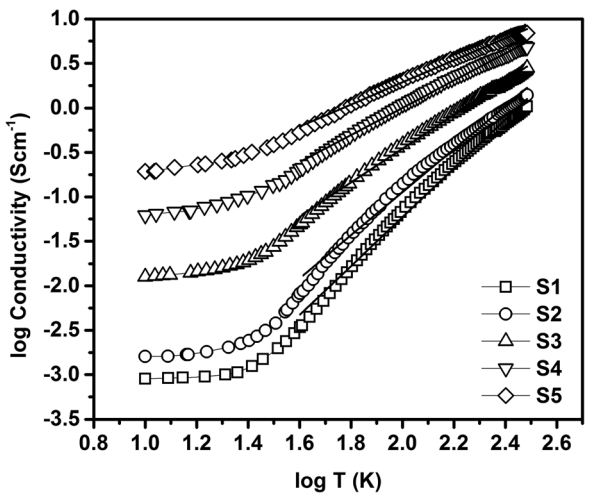

FIG. 8. Plot of log of dc conductivity (σ_{dc}) as a function of log T for S1, S2, S3, S4, and S5.

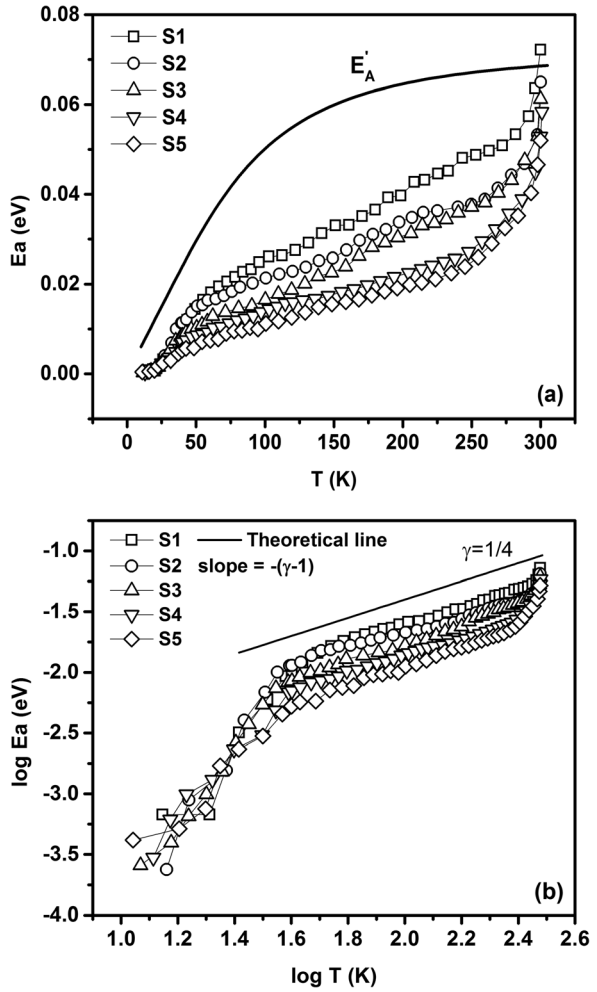

FIG. 9. (a) Activation energy (E_A) derived from Fig. 7 plotted as a function of temperature in the range of 10–300 K. As a representative result, the calculated values of activation energy E'_A are shown by a solid line in Fig. 9(a); using room temperature value of activation energy (E_A) for S1 in Eq. (4) and (b) the plot of log E_A versus log T in the temperature range of 10–300 K. The solid line corresponds to $T^{-1/4}$, slope $= -(\gamma - 1)$, $\gamma = 1/4$.

$$E_A = \gamma k_B T_0 \left(\frac{T_0}{T}\right)^{\gamma-1}, \tag{3}$$

where T_0 is the Mott's characteristic temperature and is considered as a measure of disorder, and $\gamma = 1/(d+1)$, where d is the dimensionality of hopping transport and is equal to 1, 2, or 3. It is evident from Eq. (3) that a plot of log E_A versus log T (Fig. 9(b)) should yield a slope of $-(\gamma\text{-}1)$. It can be seen from Fig. 9(b) that the activation energy shows a systematic decrease with decrease in temperature for all the samples for the whole range of measurement. A straight line corresponding to $\gamma = 1/4$ is shown in Fig. 9(b) and it appears that the value of $\gamma = 1/4$ may satisfy the variation of activation energy with temperature (40–300 K) for all the samples where hopping conduction process dominates.[17–19] It has been observed that with increase in dopant pTS concentration the temperature dependence of conductivity weakens. This can be related to the decrease in the width of barriers separating regions of higher conductivity and an increase in volume of higher conductivity phase caused by increasing dopant concentration.[33] Although the percolation effect could be the reason for the departure at lower temperatures, the authors believe that the conduction process may possibly be based on the dynamic interactions between the conductive and the non-conductive phases as has been described by Wessling.[48] However, in the low temperature region, i.e., below 40 K, the conductivity becomes less activated and the charge transport in this region may be attributed to the thermally activated tunneling through localized sites as reported earlier for other conjugated polymers.[20,30,49] Therefore, it is clearly seen that the two mechanisms dominantly govern the charge transport in PPy/C composites, i.e., 3D-VRH in the high $\sim$40–305 K and tunneling in the low temperature <40 K regions. This indicates that the VRH conduction mechanism can explain the mechanism of charge transport in PPy/C composite samples above 40 K.

It has been suggested by Holstein[50] that for an ordered material having polaronic conduction, the multiphonon process is gradually replaced at lower temperatures by the process where the only contribution to the jump frequency of the polaron is due to single optical phonon absorption and emission. The variation of activation energy for such a process is given[17,18,50] by

$$E'_A = E_A \left\{ \frac{\tanh(\hbar\omega_0/4k_BT)}{(\hbar\omega_0/4k_BT)} \right\}, \tag{4}$$

where $\hbar = h/2\pi$, $\omega_0 = 2\pi\upsilon_{ph}$, E'_A is the calculated activation energy at different temperatures by Eq. (4) using room temperature value of activation energy (E_A) and assuming the value of characteristic phonon frequency $\upsilon_{ph} \sim 10^{13}$ Hz. The theoretical plot of right hand side of Eq. (4) is shown by a solid line in Fig. 9(a) as a representative result for sample S1. The polaronic hopping conduction can give the temperature independent activation energy wherein the multiphonon process dominates. However, the temperature dependence of E'_A [Fig. 9(a)] rules out the above possibility confirming the polaronic hopping conduction through VRH in this PPy/C composite wherein single phonon process is involved.

Hence, VRH conduction model proposed by Mott and Davis[13] has been used to explain the data of the present work. For this, the temperature dependence of conductivity can be given[13,17–19,23,30,31] by the following relation:

$$\sigma(T) = \sigma_0 \exp\left[-\left(\frac{T_0}{T}\right)^{\gamma}\right], \tag{5}$$

where σ(T) is the conductivity at temperature T and σ_0 is the conductivity at infinite temperature. Plot of σ(T) versus $(1/T)^{\gamma}$ should be linear for appropriate value of γ. The plots of log σ_{dc} versus $T^{-1/2}$ and $T^{-1/4}$ for all the PPy/C composites, S1, S2, S3, S4, and S5, have been made from the data of Fig. 7. The log σ_{dc} versus $T^{-1/4}$ plot (Fig. 10) shows better linearity,[17,19] thus satisfying the condition for the application of Mott's three dimensional VRH (3D-VRH) conduction model[13] in this system.

The parameters T_0 and σ_0 of Eq. (5) can be expressed[13,18,51,52] as

$$T_0 = \frac{B_0\alpha^3}{k_B N(E_F)} \tag{6}$$

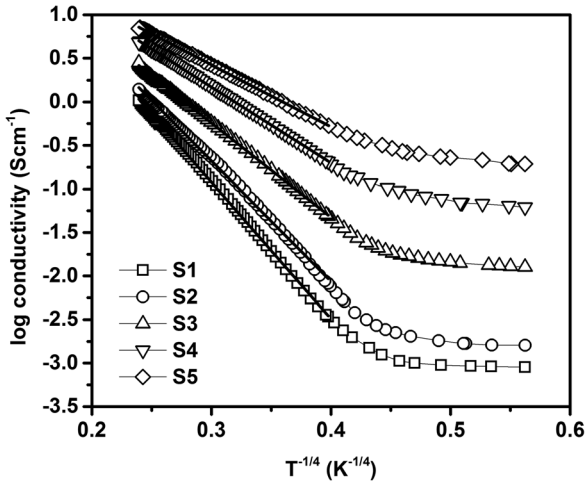

FIG. 10. Plot of log of dc conductivity (σ_{dc}) versus $T^{-1/4}$ for S1, S2, S3, S4, and S5.

and

$$\sigma_0 = e^2 R^2 \upsilon_{ph} N(E_F), \tag{7}$$

where B_0 (1.66) is a dimensionless constant, $\alpha(=1/r_p)$[13,18,19,53] is the coefficient of exponential decay of the localized states involved in the hopping process, where r_p is the polaron radius, $N(E_F)$ is the density of localized states at the Fermi level and R, the average hopping distance between the two sites is given by

$$R = \left[\frac{9}{8\pi\alpha k_B T N(E_F)}\right]^{1/4}. \tag{8}$$

The average hopping energy W can be estimated by knowing $N(E_F)$ and R by the following expression:

$$W = \frac{3}{4\pi R^3 N(E_F)}. \tag{9}$$

Mott's parameters, T_0, $N(E_F)$, R, and W evaluated by using Eqs. (6)–(9) for all the PPy/C composite samples, are given in Table II. The electron wave function localization length α^{-1} ($= r_p$) has been taken as 0.3 nm,[18,53] since the electrons are always delocalized to the extent of π-orbitals on the monomer unit. T_0 has been estimated from the slopes of log σ_{dc} versus $T^{-1/4}$ plot (Fig. 10) and is observed to decrease with increase in the conductivity (Table II). The density of states at the Fermi level $N(E_F)$ has been estimated by assuming that the electron wave function localization length α^{-1} ($=r_p$) remains independent of temperature and conductivity. The values of $N(E_F)$ lies in the range of $10^{20}-10^{21}$ cm^{-3}eV^{-1} for all the PPy/C composite samples and are in good agreement with the values reported earlier for other π-conjugated systems.[17,19,20,24,27–32] The present results are consistent with the Mott requirement that $\alpha R > 1$ and $W > k_B T$ for conductivity by hopping of charge carriers to the distant sites. The estimated values of Mott's parameters and temperature dependent activation energy suggest that Mott's 3D-VRH conduction model is appropriate for explaining the mechanism of dc electrical charge transport behavior of PPy/C composite samples. It is evident from Table II that the average hopping distance (R) and average hopping energy (W) decrease with increase in pTS concentration. Hence, with increase in the dopant concentration, the conjugation length increases[12] with a concomitant decrease in R and W, thereby stabilizing the conductive domains in the polymer matrix making this composite material suitable for electrode applications in supercapacitors.

IV. CONCLUSIONS

The temperature dependence of dc electrical conductivity of PPy/C composite samples has been explained by Mott's 3D-VRH conduction model above 40–305 K for all the samples. However, below this temperature, tunneling contribution seems to dominate. The evaluated values of Mott's parameters are in good agreement with earlier reported values for other π-conjugated polymeric systems confirming the applicability of Mott's 3D-VRH conduction model in PPy/C composite systems.

ACKNOWLEDGMENTS

The authors are thankful to the Director, National Physical Laboratory, Dr. K. S. Krishnan Marg, New Delhi for his kind permission to publish this work and Dr. R. P. Pant and Mr. J. Tawale of NPL, New Delhi for providing their experimental facilities. The authors are also thankful to Dr. S. Tripathi of CSR, Indore, India for XPS measurement. A. Kumar is thankful to Council of Scientific & Industrial Research (CSIR), New Delhi, for the award of Senior Research Fellowship. R Singh is thankful to CSIR, New Delhi for the award of Emeritus Scientist Fellowship. Financial assistance from CSIR, New Delhi under Grant No. 21(0756)/09/EMR-II is gratefully acknowledged.

[1]*Handbook of Conducting Polymers: Conjugated Polymers Theory, Synthesis, Properties and Characterization*, 3rd ed., edited by T. A. Skotheim and J. R. Reynolds (CRC Press, Taylor & Francis Group, FL, USA, 2007).
[2]*Handbook of Conducting Polymers: Conjugated Polymers: Processing and Applications*, edited by T. A. Skotheim and J. R. Reynolds (CRC Press, Taylor & Francis Group, FL, USA, 2007).
[3]S. Hotta, *in Handbook of Organic Conductive Molecules and Polymers*, edited by H. S. Nalwa (John Wiley & Sons, Inc., New York, USA, 1997), p. 309.
[4]R. Menon, *in Handbook of Organic Conductive Molecules and Polymers*, edited by H. S. Nalwa (John Wiley & Sons, Inc., New York, USA, 1997), p. 47.
[5]J.-L. Bredas, K. Cornil, F. Meyers, and D. Beljonne, in *Handbook of Conducting Polymers*, edited by T. A. Skotheim, R. L. Elsenbaumer, and J. R. Reynolds (Marcel Dekker, Inc., New York, 1998), p. 1.
[6]L.-Z. Fan and J. Maier, Electrochem. Commun. **8**, 937 (2006).
[7]H. An, Y. Wang, X. Wang, L. Zheng, X. Wang, L. Yi, L. Bai, and X. Zhang, J. Power Sources **195**, 6964 (2010).
[8]B. C. Kim, J. M. Ko, and G. G. Wallace, J. Power Sources **177**, 665 (2008).
[9]I. Sultana, M. M. Rahman, S. Li, J. Wang, C. Wang, G. G. Wallace, and H.-K. Liu, Electrochim. Acta **60**, 201 (2012).
[10]J. Wang, Y. Xu, X. Chen, and X. Du, J. Power Sources **163**, 1120 (2007).
[11]J. Wang, Y. Xu, J. Wang, and X. Du, Synth. Met. **161**, 1141 (2011).
[12]A. Kumar, R. K. Singh, H. K. Singh, P. Srivastava, and R. Singh, J. Power Sources **246**, 800 (2014).
[13]N. F. Mott and E. A. Davis, *Electronic Processes in Noncrystalline Materials*, 2nd ed. (Oxford University Press, London, 1979).

[14]S. Kivelson, Phys. Rev. Lett. **46**, 1344 (1981); Phys. Rev. B **25**, 3798 (1982).
[15]P. Kuivalainen, H. Stubb, H. Isotalo, P. Yli-Lahti, and C. Holmström, Phys. Rev. B **31**, 7900 (1985).
[16]P. Sheng, E. K. Sichel, and J. I. Gittleman, Phys. Rev. Lett. **40**, 1197 (1978); Phys. Rev. B **18**, 5712 (1978).
[17]R. K. Singh, A. Kumar, and R. Singh, J. Appl. Phys. **107**, 113711 (2010); **109**, 029901 (2011).
[18]R. K. Singh, A. Kumar, K. Agarwal, M. Kumar, H. K. Singh, P. Srivastava, and R. Singh, J. Polym. Sci. B: Polym. Phys. **50**, 347 (2012).
[19]R. K. Singh, J. Kumar, R. Singh, R. Kant, R. C. Rastogi, S. Chand, and V. Kumar, New J. Phys. **8**, 112 (2006).
[20]R. Singh, J. Kumar, R. K. Singh, S. Chand, V. Kumar, and R. C. Rastogi, J. Appl. Phys. **100**, 016106 (2006).
[21]R. Singh, A. K. Narula, R. P. Tandon, A. Mansingh, and S. Chandra, J. Appl. Phys. **79**, 1476 (1996).
[22]R. Singh, A. K. Narula, R. P. Tandon, A. Mansingh, and S. Chandra, J. Appl. Phys. **81**, 3726 (1997).
[23]R. Singh and A. K. Narula, J. Appl. Phys. **82**, 4362 (1997).
[24]S. K. Gupta, V. Luthra, and R. Singh, Bull. Mater. Sci. **35**, 787 (2012).
[25]A. J. Epstein, H. Rommelmann, R. Bigelow, H. W. Gibson, D. M. Hoffmann, and D. B. Tanner, Phys. Rev. Lett. **50**, 1866 (1983); **51**, 2020 (1983).
[26]M. Audenaert, Phys. Rev. B **30**, 4609 (1984).
[27]F. Zuo, M. Angelopoulos, A. G. MacDiarmid, and A. J. Epstein, Phys. Rev. B **39**, 3570 (1989).
[28]R. Singh, V. Arora, R. P. Tandon, S. Chandra, N. Kumar, and A. Mansingh, Polymer **38**, 4897 (1997).
[29]K. L. Yadav, A. K. Narula, R. Singh, and S. Chandra, Appl. Biochem. Biotechnol. **96**, 119 (2001).
[30]R. Singh, A. Kaur, K. L. Yadav, and D. Bhattacharya, Curr. Appl. Phys. **3**, 235 (2003).
[31]I. Youm, M. Cadène, and D. Laplaze, J. Mater. Sci. Lett. **14**, 1712 (1995).
[32]J. Kumar, R. K. Singh, S. Chand, V. Kumar, R. C. Rastogi, and R. Singh, J. Phys. D: Appl. Phys. **39**, 196 (2006).
[33]D. T. Glatzhofer, J. Ulański, and G. Wegner, Polymer **28**, 449 (1987).
[34]R. Menon, C. Yoon, D. Moser, and A. J. Heeger, *in Handbook of Conducting Polymers*, 2nd ed., edited by T. A. Skotheim, R. L. Elsenbaumer, and J. R. Reynolds (Marcel Dekker, Inc., New York, 1998), p. 27.
[35]C. Yang, P. Liu, and T. Wang, ACS Appl. Mater. Interfaces **3**, 1109 (2011).
[36]H. S. Nalwa, Phys. Rev. B **39**, 5964 (1989).
[37]X. Liu, K. G. Neoh, L. Cen, and E. T. Kang, Biosens. Bioelectron. **19**, 823 (2004).
[38]F. Fusalba and D. Bélanger, J. Phys. Chem. B **103**, 9044 (1999).
[39]C.-C. Hu and X.-X. Lin, J. Electrochem. Soc. **149**, A1049 (2002).
[40]F. Beck, Electrochim. Acta **33**, 839 (1988).
[41]R. Erlandsson, O. Inganäs, I. Lundström, and W. R. Salaneck, Synth. Met. **10**, 303 (1985).
[42]H.-T. Lee and Y.-C. Liu, Polymer **46**, 10727 (2005).
[43]P. D. C. King, T. D. Veal, P. H. Jefferson, C. F. McConville, T. Wang, P. J. Parbrook, H. Lu, and W. J. Schaff, Appl. Phys. Lett. **90**, 132105 (2007).
[44]J. C. Scott, P. Pfluger, M. T. Krounbi, and G. B. Street, Phys. Rev. B **28**, 2140 (1983).
[45]R. Singh and A. K. Narula, Synth. Met. **82**, 245 (1996).
[46]F. Moraes, J. Chen, T.-C. Chung, and A. J. Heeger, Synth. Met. **11**, 271 (1985).
[47]M. Binder, R. J. Mammone, and N. E. Schlotter, Synth. Met. **39**, 215 (1990).
[48]B. Wessling, Polym. Eng. Sci. **31**, 1200 (1991).
[49]R. S. Kohlman and A. J. Epstein, in *Handbook of Conducting Polymers*, 2nd ed., edited by T. A. Skotheim, R. L. Elsenbaumer, and J. R. Reynolds (Marcel Dekker, Inc., New York, 1998), p. 85.
[50]T. Holstein, Ann. Phys. **8**, 343 (1959).
[51]R. Singh, R. P. Tandon, G. S. Singh, and S. Chandra, Philos. Mag. B **66**, 285 (1992).
[52]D. K. Paul and S. S. Mitra, Phys. Rev. Lett. **31**, 1000 (1973).
[53]D. S. Maddison and T. L. Tansley, J. Appl. Phys. **72**, 4677 (1992).